Theoret. Comput. Fluid Dynamics (1991) 3: 1–13

Theoretical and Computational Fluid Dynamics

Near-Wall Turbulence Closure Modeling Without "Damping Functions"

P.A. Durbin

Center for Turbulence Research,
Moffett Field, CA 94035, U.S.A.

Communicated by John Lumley

Received 18 June 1990 and accepted 22 January 1991

Abstract. An elliptic relaxation model is proposed for the strongly inhomogeneous region near the wall in wall-bounded turbulent shear flow. This model enables the correct kinematic boundary condition to be imposed on the normal component of turbulent intensity. Hence, wall blocking is represented. Means for enforcing the correct boundary conditions on the other components of intensity and on the $k-\varepsilon$ equations are discussed. The present model agrees quite well with direct numerical simulation (DNS) data. The virtue of the present approach is that arbitrary "damping functions" are not required.

1. Introduction

A near-wall turbulent flow can be divided into two regions: the inner region scales on a viscous length, such as ν/u_* or the Kolmogoroff scale $(\nu^3/\varepsilon)^{1/4}$; and the outer region scales on a flow dimension, such as a channel half-width or a boundary-layer thickness. The peak turbulent energy, and the peak in production of turbulence both occur within the inner region. If we are concerned with modeling wall-bounded turbulent shear flow, it is essential to represent this region.

To date, single-point second-order closure models have been based on quasi-homogeneous approximations. They fail badly near the wall, in the strongly non-homogeneous inner region. The remedy taken by many investigators is to introduce *ad hoc* "damping functions" which are adjusted to make the model fit experimental or computational data (Patel *et al.*, 1985; Hanjalic and Launder, 1976). Table 1 of Patel *et al.* and Table 2 of Shih (1990) list some of the various functions which have been used. These functions are quite arbitrary, their common feature being that they involve exponentials. The use of exponentials dates back to van Driest's (1956) model for viscous damping of mixing lengths. However, the models in which these damping functions are employed contain viscous terms explicitly. The rationale behind the damping functions must differ from that given by van Driest.

Figure 1 might help to clarify the role of damping functions and to explain the motivation for this paper. This figure was constructed from numerical simulation data (Kim private communication). The solid line shows an evaluation of the eddy viscoscity as defined by

$$\nu_t = -\frac{\overline{uv}}{\partial_y U}.$$

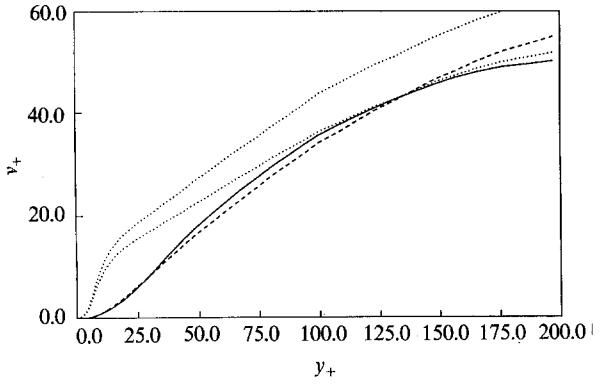

Figure 1. Exact eddy viscoscity (solid line) compared with the formulas used in the $k-\varepsilon$ (dotted line) and $k-\varepsilon-v$ (dashed line) models. These curves were computed using DNS data.

In the usual $k-\varepsilon$ model, it is assumed that ν_t can be approximated by

$$\nu_t = C_\mu kT,$$

where $T = k/\varepsilon$. The usual value of C_μ is 0.09. The dotted lines show evaluations of this expression with $C_\mu = 0.09$ and 0.075. The latter is included to make it clear that the $k-\varepsilon$ models does not fail near the wall ($y_+ < 100$) simply because C_μ is too high: the $k-\varepsilon$ model fails because k^2/ε has the wrong profile as a function of y_+. The "damping function" is simply a correction function which is defined to be the ratio of the solid to the dotted curve. Thus, when the $k-\varepsilon$ viscoscity is multiplied by the correction function it will give the correct profile of ν_t. This curve-fitting approach can sometimes be effective for engineering calculations. It is unattractive, however, to use a model which is fundamentally incorrect, and then to correct it by introducing an arbitrary function. At a basic level, the problem is that the $k-\varepsilon$ formula is isotropic, while near-wall turbulence is strongly anisotropic.

The dashed line in Figure 1 is the $k-\varepsilon-v$ formula

$$\nu_t = C_\mu \overline{v^2} T,$$

with T as previously, and with the present value of $C_\mu = 0.2$. This curve follows the solid line closely in the near wall region. The $k-\varepsilon-v$ formula represents the anisotropy of near-wall transport processes; it is quite gratifying that the principle of tensoral invariance (Lumley, 1978) confirms that $\overline{v^2}$ rather that k is the appropriate velocity scale to use. Thus, it seems that if we can model $\overline{v^2}$ satisfactorily, the need for a correction function can be avoided. A $k-\varepsilon-v$ model is described in this paper.

The observation made by Figure 1 is that the suppression of ν_t near the wall is largely accounted for by the $\overline{v^2}$ scaling. This suggests that a primary objective of damping in closure models is to represent kinematic blocking by the wall (Hunt and Graham, 1978; Thomas and Hancock, 1977; Launder, 1986). The velocity component normal to the wall, v at present, must be inviscidly brought to zero at the wall. Very near to the wall, all velocity components are viscously brought to zero, but the inviscid blocking of v has an effect at considerably greater distances from the wall (Hunt and Graham). Blocking is associated with "image" vorticity, and cannot be explicitly incorporated into a *single*-point closure. However, we might approach the blocking problem by noting that blocking is governed by an *elliptic* partial differential equation (i.e., Poisson's equation). This implies that nonlocal effects in strongly nonhomogeneous turbulent flow should be introduced by an elliptic model. In incompressible flow, pressure fluctations obey an elliptic equation, so it seems natural to introduce ellipticity into terms which represent pressure–velocity correlations in the Reynolds stress equations. It should be remarked, however, that in the linear analysis of wall blocking by Hunt and Graham, the pressure field vanishes; wall blocking is not due to pressure–velocity correlations. Nevertheless, it turns out, as will be seen, that the kinematic constraints due to blocking can be introduced through an elliptic pressure–velocity model.

The wall effect on pressure fluctuations has been discussed previously by Launder and coworkers (Gibson and Launder, 1978). This work addresses the dynamical effect of boundaries, through their influence on the pressure field. In common with the present work, Gibson and Launder address an

elliptic phenomenon associated with boundary conditions. However, the effect of boundaries on pressure fluctuations is rather different from kinematic blocking. The latter is an immediate consequence of the boundary condition on v; the former affects the evolution of $\overline{v^2}$ by altering the source term in the $\overline{v^2}$ equation. The difference between kinematic and dynamic wall effects is quite important; and it is made quite clear by exact analyses such as that by Hunt and Graham (1978). In a single-point closure model it is not so easy to distinguish the effects, although both should be represented. Here the distinction between dynamic and kinematic effects is associated with that between particular and homogeneous solutions to the model equations for $\overline{v^2}$.

Current quasi-homogeneous closure models (such as $k-\varepsilon$ or second-order moment closures) might be described as parabolic relaxation models. The evolution of turbulent velocity moments is represented by parabolic diffusion operators. In the algebraic limit of Rodi (1976) these models assume an eddy diffusion form. The parabolic operators can be thought of as governing the relaxation in time to something like this eddy diffusion equilibrium. The above discussion suggests that strong nonhomogeneity might be modeled by elliptic relaxation. By introducing this type of relaxation the need for damping functions can be obviated. In this case the relaxation is in space rather than time.

In this paper, such a model is developed for channel flow. The direct numerical simulation (DNS) data of Kim (private communication; Kim *et al.*, 1987) is used to adjust closure constants. This flow is ideal for developing nonhomogeneous closure models because it is statistically stationary and nonhomogeneous in only one direction, y. The model equations then reduce to ordinary differential equations. Additionally, in channel flow the tensoral invariance arguments described by Launder *et al.* (1975) lead to a simple pressure-strain model which allows us to formulate a closed set of equations for k, ε, and $\overline{v^2}$. These are uncoupled from the other components of the Reynolds stress tensor.

Another consideration in near-wall modeling is that the dissipation tensor is quite anisotropic near the wall. Rotta's (1951) model

$$\varepsilon_{ij} = \frac{\overline{u_i u_j}}{k}\varepsilon \tag{1}$$

seems to describe this anisotropy (Mansour *et al.*, 1988). The relaxation from (1) to an isotropic form away from the wall can be described by combining the dissipation anisotropy, $\varepsilon_{ij} - 2/3\delta_{ij}\varepsilon$, with the velocity–pressure gradient correlation, as suggested by Lumley (1978). By doing so, the need for a dissipation rate damping function (f_s in Hanjalic and Launder (1976)) is also obviated.

An issue which has been discussed in the literature (Patel *et al.*, 1985) but not resolved, is the correct boundary conditions for the ε equation. Taken together, the k and ε equations are fourth order in derivatives of k. The correct viscous boundary condition is that k and its normal derivative are zero at stationary walls: for instance, in channel flow k and $d_y k$ are zero at both walls. In general, boundary conditions cannot be imposed on ε. In steady channel flow the boundary conditions on k can be enforced through an integral constraint on ε; otherwise, the coupled k and ε equations should simply be solved as a fourth-order system.

2. The $k - \varepsilon - \overline{v^2}$ Model

We use the standard k and ε equations (Patel *et al.*, 1985). For steady turbulent channel flow these are

$$\begin{aligned} d_y\left(\nu + \frac{\nu_t}{\sigma_k}\right) d_y k &= \varepsilon - \nu_t (d_y \bar{U})^2, \\ d_y\left(\nu + \frac{\nu_t}{\sigma_\varepsilon}\right) d_y \varepsilon &= \frac{C_{\varepsilon_2}\varepsilon - C_{\varepsilon_1}\nu_t (d_y \bar{U})^2}{T}, \end{aligned} \tag{2}$$

where C_{ε_1}, C_{ε_2}, σ_k, and σ_ε are empirical model constants and T is a time-scale for the evolution of ε. If lengths are nondimensionalized by the channel half-height and velocities by the friction velocity, then the mean flow satisfies

$$(\nu + \nu_t)\, d_y \bar{U} = 1 - y. \tag{3}$$

The wall is at $y = 0$ and the center of the channel is at $y = 1$. In nondimensional terms ν is one over

the Reynolds number ($\nu = \nu_*/u_* d \equiv R_\tau^{-1}$, where ν_* is the dimensional viscoscity and u_* is the friction velocity).

In these equations ν_t is the eddy viscoscity. If we represent turbulent transport of a quantity φ by a diffusion process:

$$\partial_i(\overline{u_i\varphi}) \approx \partial_i \nu_{ij} \partial_j \overline{\varphi}$$

with $\nu_{ij} = C_\mu \overline{u_i u_j} T$, then for channel flow the tensorally correct eddy viscoscity is

$$\nu_t \equiv \nu_{22} = C_\mu \overline{v^2} T. \tag{4}$$

$\overline{v^2}$ is the appropriate velocity scale to use.

The time-scales in (2) and (4) are assumed to be equal. They represent the decorrelation rate of turbulent eddies—the diffusive time-scale in (4) is usually understood to be the Lagrangian time-scale of the turbulence. The interpretation of T in (2) is not as clear. It is not the time-scale of the small eddies; it is the time-scale on which dissipation evolves.

Away from the wall $T = k/\varepsilon$ is a reasonable estimate. However, as $y \to 0$, $k \to 0$ while $\varepsilon > 0$. Hence, at some point k/ε will become less than the Kolmogoroff scale $(\nu/\varepsilon)^{1/2}$. Of course, the eddy time-scale cannot be less than the Kolmogoroff scale. Therefore, we use

$$T = \max\left(\frac{k}{\varepsilon}, C_T\left(\frac{\nu}{\varepsilon}\right)^{1/2}\right) \tag{5}$$

as an expression that remains valid near walls. This prevents a singularity at $y = 0$ in the ε equation (2).

The constant C_T in (5) can be estimated as follows: at $y = 0$, (2) with (4) and (5) becomes

$$\nu d_y^2 \varepsilon = \frac{C_{\varepsilon_2} \varepsilon^{3/2}}{C_T \nu^{1/2}}.$$

Mansour *et al.* (1988) give $\varepsilon = 0.166 R_\tau$ at $y = 0$, and their Figure 6 gives $D_\varepsilon \equiv \nu d_y^2 \varepsilon = 0.02 R_\tau^2$ at $y = 0$. These values, with a typical value of $C_{\varepsilon_2} = 1.9$ give $C_T = 6.4$. In calculations C_T was varied by a factor of 2, with no appreciable affect on the model: the value $C_T = 6$ was deemed satisfactory. k/ε only becomes less than the Kolmogorov scale when y_+ is less than about 5: this is why C_T is such an insensitive parameter and, indeed, why it is inconsequential whether (5) or some other interpolation formula is used.

In a channel flow k and $d_y k$ are zero at the walls, as a consequence of the no-slip boundary condition. Symmetry allows the flow to be solved in a half channel with

$$\begin{aligned} k = d_y k = 0 \qquad &\text{at} \quad y = 0, \\ d_y k = d_y^3 k = 0 \qquad &\text{at} \quad y = 1, \end{aligned} \tag{6}$$

$y = 1$ is the centerline of the channel. If ε were eliminated between equations (2) a fourth-order equation for k would be obtained, and conditions (6) could be imposed. Alternatively, (6) will be satisfied if (2) are solved subject to

$$\begin{aligned} d_y k = d_y \varepsilon = 0 \qquad &\text{at} \quad y = 1, \\ k = 0 \qquad &\text{at} \quad y = 0, \\ \int_0^1 \varepsilon \, dy = \int_0^1 \nu_t (d_y \bar{U})^2 \, dy. & \end{aligned} \tag{7}$$

The last condition will make $d_y k = 0$ at the wall. It also sets the total rate of energy dissipation equal to the total rate of production, thus expression the overall energy balance. Other investigators have imposed conditions on ε at $y = 0$. These conditions must violate the energy balance, and do not ensure satisfaction of conditions (6). The integral constraint on ε only applies to parallely, steady flow. More generally, the $k - \varepsilon$ model must be solved as a fourth-order system so that correct boundary conditions can be imposed. For numerical computation, block tridagonal finite differencing can be used to solve simultaneously for k and ε, thereby enabling the imposition of (6). The present

computations were first done with the integral constraint, then repeated with the more general block tridiagonal method: of course the results differ only in the precise value of the truncation error.

The model equation to be used for $\overline{v^2}$ is

$$d_y\left(\nu + \frac{\nu_t}{\sigma_k}\right) d_y\overline{v^2} - \overline{v^2}\frac{\varepsilon}{k} = -\wp_{22}, \tag{8}$$

where the anisotropic dissipation (1) appears on the left-hand side. This model is discussed further in Appendix B. Comparison to the exact equation for $\overline{v^2}$ (Hanjalic and Launder's (2.1)) shows that

$$\wp_{22} = -2\frac{\overline{v\partial_y p}}{\rho} - \varepsilon_{22} + \overline{v^2}\frac{\varepsilon}{k}, \tag{9}$$

where $\varepsilon_{22} = 2\nu|\nabla v|^2$. Thus, $\wp_{22}$ is a combination of pressure–velocity correlation and anisotropic dissipation. The generalization of (9) to a tensor form is discussed in Appendix B.

Taylor series expansion shows that $k \to (1/2\nu)\varepsilon y^2$ and $\wp_{22} = O(y^2)$ as $y \to 0$ (Mansour *et al.*, 1988). Thus as $y \to 0$, (8) becomes

$$\nu d_y^2\overline{v^2} - 2\nu\frac{\overline{v^2}}{y^2} = O(y^2). \tag{10}$$

This shows that $y = 0$ is a regular singular point of (8). The solution to (10) is

$$\overline{v^2} = Ay^2 + \frac{B}{y} + O(y^4). \tag{11}$$

The first two terms are homogeneous solutions and the $O(y^4)$ term is a particular solution. The viscous and *kinematic* (or blocking) conditions show that $\overline{v^2} = O(y^4)$ as $y \to 0$. Hence, the boundary condition to (10) is that the homogeneous solutions in (11) must vanish; or that $A = B = 0$.

The regular singular point of (10) caused some numerical difficulty. To avoid this, ε/k was replaced by $1/T$ in (8) so that $y = 0$ was not exactly a singular point. The boundary condition remains that the homogeneous solutions to (8) vanish and the particular solution is then $O(y^4)$.

It might now be objected that (4) makes ν_t be $O(y^4)$ instead of correctly being $O(y^3)$ in the k, v, and $\bar{U}$ equations and $O(y^2)$ in the ε equation. Our response to such an objection is that at small y, where this ordering argument is valid, the *total* viscoscity $\nu + \nu_t$ is represented *correctly* as $O(1)$. By their nature, closure models will fail to satisfy many of the constraints met by actual turbulence statistics. To judge which constraints are crucial, we must decide which are the dominant terms in each equation. Getting the dominant behavior correctly is a sufficient challenge.

It also is seen in Figure 1 that, for $y^+ < 25$, equation (4), with its $O(y^4)$ behavior, agrees excellently with the exact formula, despite the latter being $O(y^3)$. It seems that in this case the Taylor series constraint is not compelling, aside from the fact that both curves must be flat at the origin.

The $\wp_{22}$ Model

By eliminating the homogeneous solutions to (8) the correct near-wall behavior $\overline{v^2} \to O(y^4)$ can be obtained. This imposes two conditions on the second-order ordinary differential equation (8). The symmetry condition $d\overline{v^2}/dy = 0$ at $y = 1$ cannot additionally be imposed. However, that condition will be satisfied if the source term $\wp_{22}$ satisfies an integral constraint analogous to that imposed on ε in (7):

$$\int_0^1 \wp_{22}\, dy = \int_0^1 \frac{\overline{v^2}\varepsilon}{k}\, dy. \tag{12}$$

In order to satisfy such a constraint, an equation for $\wp_{22}$ is required. It is argued in Appendix A and in the introduction that such an equation should be an elliptic relaxation model, which represents nonlocal effects such as wall blocking.

As $y \to 0$, $\wp_{22}$ as defined in (9) tends to $O(y^2)$ and hence $f_{22} \equiv \wp_{22}/k$ is $O(1)$. Indeed, quasi-homogeneous models such as that of Launder *et al.* (1975) (LRR)—which is incorporated into the present nonhomogeneous model—suggest that $\wp_{22}$ normalized by k is an appropriate function to

work with. Here, this normalization enforces the requirement that $\wp_{22} = O(y^2)$. Our elliptic model is

$$\begin{aligned} \wp_{22} &= kf_{22}, \\ L^2 d_y^2 f_{22} - f_{22} &= -\frac{\Pi_{22}}{k} - \frac{[\overline{v^2}/k - \frac{2}{3}]}{T}, \end{aligned} \tag{13}$$

where Π_{22} is the LRR model (the unsimplified version) for the 2-2 component of pressure-strain:

$$\frac{\Pi_{22}}{k} = \frac{C_1}{T}\left(\frac{2}{3} - \frac{\overline{v^2}}{k}\right) + C_2 \frac{v_t}{k}(d_y \bar{U})^2. \tag{14}$$

In (13) L is a length-scale. In the homogeneous limit (or far from the wall—in y_+ units) (13) gives

$$\wp_{22} \to \Pi_{22} + (\overline{v^2} - \tfrac{2}{3}k)\frac{\varepsilon}{k}. \tag{15}$$

With this, (8) becomes

$$d_y\left(\nu + \frac{\nu_t}{\sigma_k}\right) d_y \overline{v^2} - \tfrac{2}{3}\varepsilon = -\Pi_{22} \tag{16}$$

which is the usual quasi-homogeneous model, with isotropic dissipation. Thus, (13) provides for elliptic relaxation of the pressure–velocity and anisotropic dissipation terms.

The constraints which determine a unique solution to (13) are

$$\begin{aligned} \int_0^1 kf_{22}\, dy &= \int_0^1 \frac{\overline{v^2}\varepsilon}{k} dy, \\ d_y f_{22} &= 0 \qquad \text{at} \quad y = 1. \end{aligned} \tag{17}$$

These ensure that $d_y \overline{v^2} = d_y^3 \overline{v^2} = 0$ at $y = 1$. As discussed below (7), the integral constraint applies only to parallel, steady flow. More generally, the $\overline{v^2} - \wp_{22}$ equations provide a fourth-order system on which the boundary conditions for $\overline{v^2}$ can be imposed.

For the length scale L we use $C_L k^{3/2}/\varepsilon$ away from the wall. As in the case of T, this can become smaller than the Kolmogoroff scale $(\nu^3/\varepsilon)^{1/4}$ near the wall, so again the Kolmogoroff scale provides a lower bound:

$$L = C_L \max\left(\frac{k^{3/2}}{\varepsilon}, C_\eta\left(\frac{\nu^3}{\varepsilon}\right)^{1/4}\right). \tag{18}$$

C_L and C_η are empirical constants. Although log-region behavior gives an estimate of $C_L \approx 0.1$, we have used a value of $C_L = 0.17$ based solely on fitting our model to DNS data. On the same basis we use $C_\eta = 80$. Thus, near the wall $L = C_L C_\eta (\nu^3/\varepsilon)^{1/4} \approx 14(\nu^3/\varepsilon)^{1/4}$. This value of 14 Kolmogoroff scales does not seem unreasonable: if we expect model constants to be $O(1)$, 14 may seem large, but the spacing of wall streaks is $O(100)$ Kolmogoroff scales (Kim *et al.*, 1987), so large constants have some precedent in the near-wall region. Our model is sensitive to the value of C_η (unlike the insensitivity to C_T) and the value of 80 is needed to obtain adequate blocking: in other words, if C_η is much smaller than 80, then the predicted $\overline{v^2}$ will be too large near the wall.

LRR give the values $C_2 = \frac{4}{11}$, $C_1 = 1.5$ for the constants in (14) (in their notation, the present C_2 is $(24 - 30c_2)/33$ with the recommended value of $c_2 = 0.4$, see Hanjalic and Launder's (2.3)). These were obtained by fitting data on homogeneous turbulence. When the model (2), (14), and (16) is evaluated in the log-region, where $\varepsilon = 1/(\kappa y)$ and $d_y \bar{U} = 1/(\kappa y)$, we find that k and $\overline{v^2}$ are constants satisfying

$$\begin{aligned} C_\mu \overline{v^2} k &= 1, \\ C_2 - C_1\left(\frac{\overline{v^2}}{k} - \frac{2}{3}\right) &= \frac{2}{3}. \end{aligned} \tag{19}$$

(Of course this log-region structure only exists as a common asymptote to the inner and outer regions when $R_\tau \to \infty$.) With the LRR constants we obtain $\overline{v^2}/k = 0.46$, which is too large. If both constants are reduced by 20% to $C_2 = 0.3$ and $C_1 = 1.2$, then $\overline{v^2}/k = 0.36$, which is more in line with experi-

mental and computational data (Townsend, 1976; Kim *et al.*, 1987). These are the values which were used in the present calculations. The issue of model constants deserves further attention: actually, LRR introduced a function of y, which had the effect of reducing C_1 and C_2 near the wall, for the reason just given—this approach was abandoned by Hanjalic and Launder. The log-region analysis also shows that the von Karman constant κ is given by

$$\kappa^2 = \frac{(C_{\varepsilon_2} - C_{\varepsilon_1})\sigma_\varepsilon}{k}. \tag{20}$$

This connection between κ and the *difference* between the ε-equation constants is well known (Launder *et al.*, 1975). The present values of these constants were adjusted to fit computational data. As will be seen, in order to fit the data,we were forced to make the difference between C_{ε_2} and C_{ε_1} smaller than it is usually taken to be. This was done with great reluctance, since the standard values of these constants have, in the course of time, been adjusted to give reasonable predictions for a variety of flows. However, the standard $k-\varepsilon$ model cannot predict near-wall behavior, and it is common practice to allow model constants to differ from their quasi-homogeneous values: the usual rationale is that the model constants ought to depend on a *local* turbulent Reynolds number (Hanjalic and Launder, 1976). There is little question that the closure constants in the ε equation should be functions of turbulent Reynolds number—or, more correctly, that terms have been dropped from the ε equation which are significant near to walls. At the present stage, our objective has been to show that a model which incorporates nonlocal elliptic effects will give reasonable predictions, without a need for damping functions. For this reason an attempt was made to keep the model relatively simple. Improvements to the model will undoubtably be made in the course of time.

3. Channel Flow Calculations

The model (2), (8), and (13) was solved numerically by adding time-derivatives to the left-hand sides of (2) and (8), forming implicit, tridiagonal difference equations, and solving them iteratively until a steady state was reached. Computations were stopped when they had converged to four of five figures; single precision arithmetic was used.

The model constants were fiddled with in order to see if reasonable agreement with the DNS data could be obtained without damping functions. Figure 2(a)–(c) shows calculations of k, $\overline{v^2}$, $\bar{U}$, and ε at $R_\tau = 395$. For these calculations $C_{\varepsilon_1} = 1.7$, $C_{\varepsilon_2} = 2.0$, $\sigma_\varepsilon = 1.6$, $\sigma_k = 1.3$, and $c_\mu = 0.2$. The plots are in wall units: thus $y_+ = yR_\tau$ and $\varepsilon_+ = \varepsilon/R_\tau$. The closure constants were adjusted by comparison to these data at $R_\tau = 395$. It is unavoidable that a semiempirical model will contain constants to adjust; however, when the number of constants is finite (and small) the differential model equations determine the profile of turbulence statistics. This contrasts to the infinite degrees of freedom in the damping function, which are used to fit an entire mean velocity profile.

Good agreement between the model and data has been obtained, the most glaring descrepancy being that the slope in the log-linear plot of $\bar{U}$ is too high in the log-region. This is probably because $C_{\varepsilon_2} - C_{\varepsilon_1}$ is too small; see (20). If this difference were increased the centerline velocity (which is a friction factor in the present normalization) would fall below the data. The satisfying feature of these figures is that the data has been fit without using arbitrary damping functions. The quasi-homogeneous model would underpredict the kinetic energy peak and centerline velocity by about 50%.

A key to predicting the data is getting the near-wall behavior of $\overline{v^2}$ right. The $\wp_{22}$ model is required for this purpose. The physical interpretation of $\wp_{22}$ is a bit nebulous (see Appendix A). It should be appreciated that (9) does not completely define $\wp_{22}$. The integral constraint (12) is an essential property because it enables the boundary conditions on $\overline{v^2}$ to be satisfied. Thus, $\wp_{22}$ represents a combination of pressure–velocity correlation, anisotropic dissipation, and wall blocking. Figure 3 shows $\wp_{22}$ along with the right-hand side of (13) multiplied by k. Away from the wall $\wp_{22}$ relaxes to its quasi-homogeneous form (15), and the two curves in Figure 3 overlap. Closer to the wall $\wp_{22}$ falls below the curve showing the source term. This is reminiscent of the comparison in Figure 27 of Mansour *et al.* (1988) between the LRR model and DNS data on pressure-strain. The data fall well

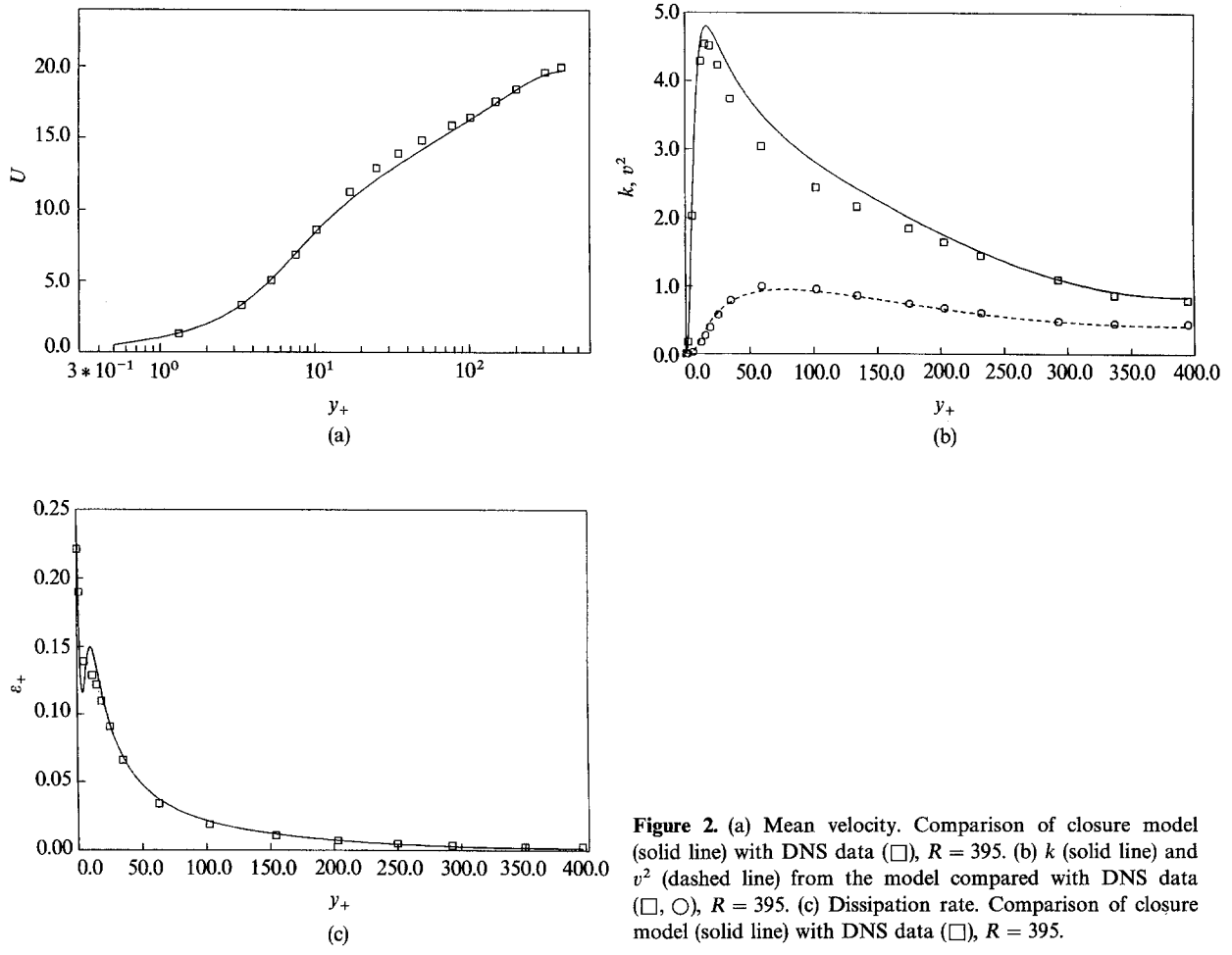

Figure 2. (a) Mean velocity. Comparison of closure model (solid line) with DNS data (□), $R = 395$. (b) k (solid line) and v^2 (dashed line) from the model compared with DNS data (□, ○), $R = 395$. (c) Dissipation rate. Comparison of closure model (solid line) with DNS data (□), $R = 395$.

below the quasi-homogeneous LRR model as the wall is approached. It seems, then, that the idea of elliptic relaxation can account for the large descrepancy between the LRR model and the data that Mansour *et al.* observed.

Figure 4 shows a calculation at the lower Reynolds number of 180. The mean velocity is predicted as well as at the higher Reynolds number, but the kinetic energy is overpredicted away from the wall. Clearly, the model does not do as well at the lower Reynolds number: this is not surprising, as the closure constants were based on the higher Reynolds number data. Shih (1990) compared five

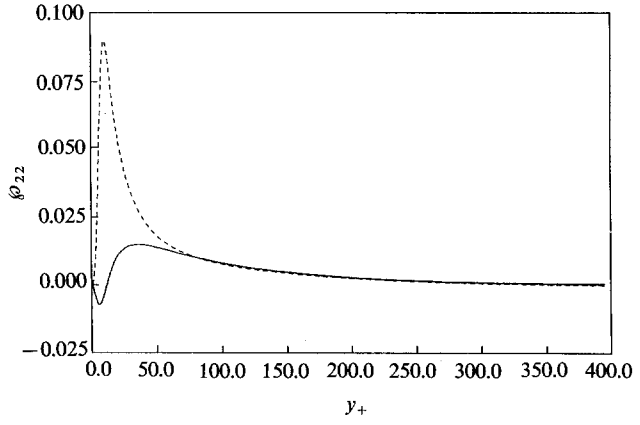

Figure 3. The solution for $\wp_{22}$ is shown by the solid line and the dashed line shows the source term of (13) multiplied by k.

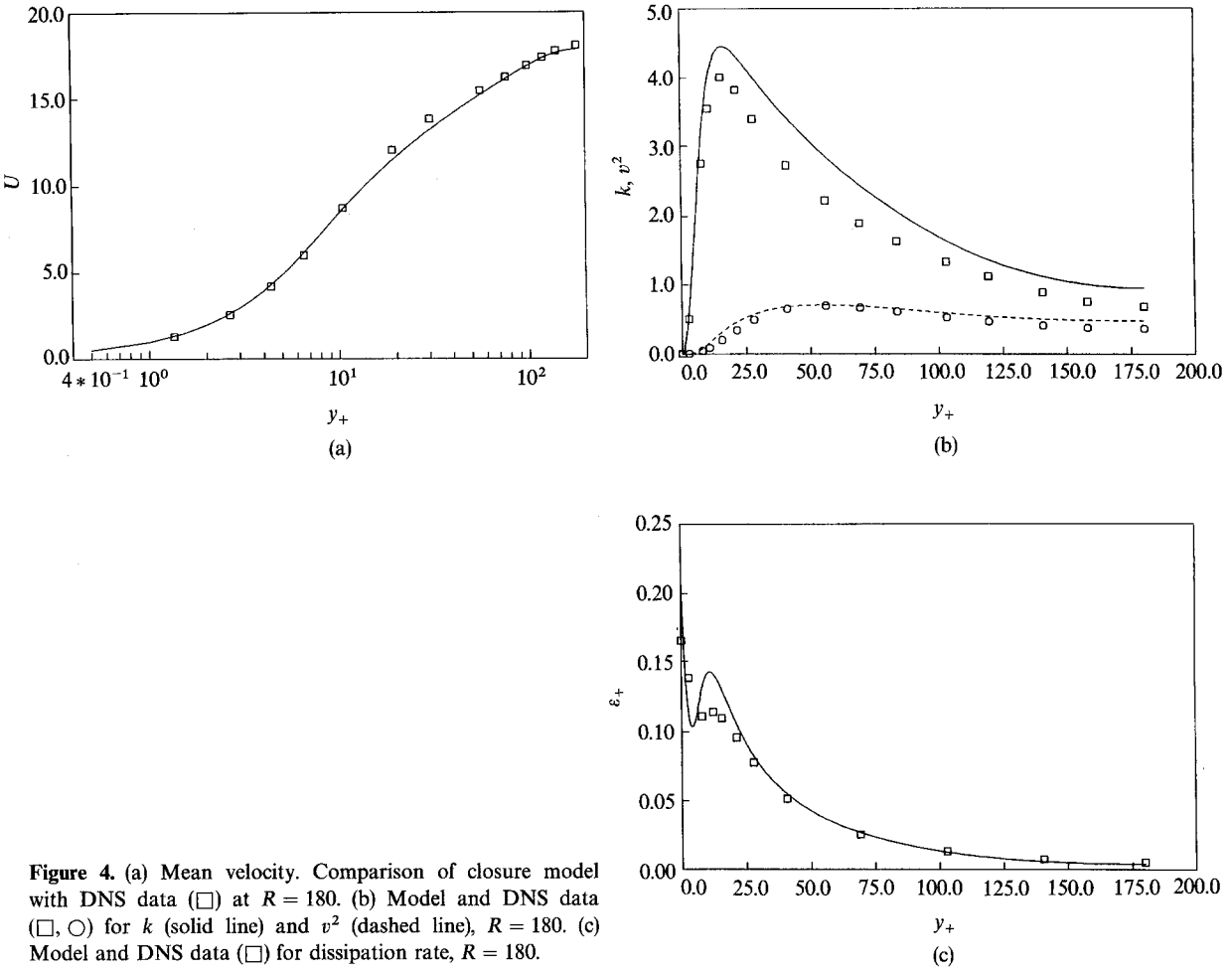

Figure 4. (a) Mean velocity. Comparison of closure model with DNS data (□) at $R = 180$. (b) Model and DNS data (□, ○) for k (solid line) and v^2 (dashed line), $R = 180$. (c) Model and DNS data (□) for dissipation rate, $R = 180$.

damping function models to this same Re = 180 data, and in every case found that the kinetic energy was overpredicted away from the wall by an amount similar to that shown in Figure 4(b): this was true even of a damping function which he had adjusted to fit the eddy viscoscity for these data. In most cases the damping-function models were in poorer agreement with the mean flow than the present model. Of course, it should be recognized that those functions were adjusted to fit other data, while the present constants were obtained from DNS channel flow data.

At both Reynolds numbers the model profile of ε has a wiggle near the wall which is larger than the data show. This is possibly because C_{ε_1} is a bit high, making the production term too large in the ε equation. The sharp peak of ε at $y = 0$ occurs because the first term on the right-hand side of the ε equation (2) is dominant at small y: when $y_+ < 5$ the Kolmogoroff scale is the greater in (5), so that

$$d_{y_+}^2 \varepsilon_+ = \frac{C_{\varepsilon_2}}{C_T} \varepsilon_+^{3/2}.$$

The solution to this, having $\varepsilon = \varepsilon_0$ at $y_+ = 0$ and $\varepsilon \to 0$ as $y_+ \to \infty$, is

$$\frac{\varepsilon}{\varepsilon_0} = \left(1 + \sqrt{\frac{C_{\varepsilon_2}}{20 C_T}} \varepsilon_0^{1/4} y_+\right)^{-4}.$$

With the present constants and $\varepsilon_0 \approx 0.2$ this last expression becomes $(1 + 0.09 y_+)^{-4}$. This falls off a bit more rapidly than the peaks in the figures, but it essentially explains the behavior of ε near the wall.

Finally, in Figure 5 the present model has been solved with the "standard" ε-equation constants (Patel *et al.*, 1985; $C_{\varepsilon_1} = 1.44$, $C_{\varepsilon_2} = 1.92$, $\sigma_k = 1.0$, $\sigma_\varepsilon = 1.3$) and is shown by the dashed curve. The

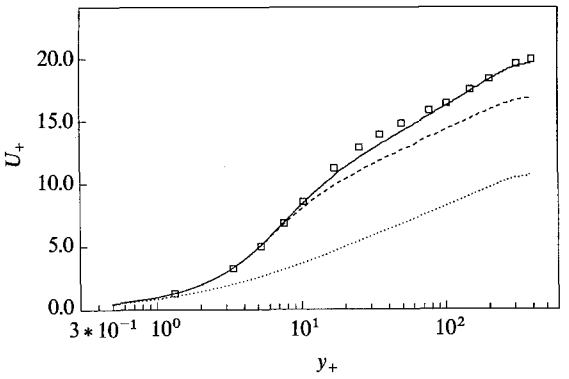

Figure 5. Computations with the present constants (solid line), with the "standard" ε-equation constants (dashed line), and with the standard $k-\varepsilon$ model (dotted line).

solid curve and data are as in Figure 2(a). For comparison, the standard $k-\varepsilon$ model with no damping is included as the dotted curve. This last curve shows how essential it is to model the blocking effect. The dashed curve underpredicts the centerline velocity. This is why it was necessary to increase C_{ε_1} above its standard value. One rationalization for this departure from quasi-homogeneous values is that the ε equation contains terms which would vanish under local isotropy, but which are significant near boundaries. These are the terms P_ε^1 and P_ε^2 is Mansour *et al.* (1989): their importance near to the wall is demonstrated in that paper.

4. Conclusion

The primary objective of this paper has been to propose a method for modeling the strongly nonhomogeneous near-wall region. A case has been made that kinematic blocking is an important phenomenon, which has an effect at significant distances from the wall (maybe out to $y_+ \approx 100$). Wall blocking is a consequence of the boundary condition on $\overline{v^2}$, and so we have made boundary conditions an issue here. Thus, the $\overline{v^2}-\wp_{22}$ and $k-\varepsilon$ equations provide fourth-order systems to which the appropriate boundary conditions can be applied. As in all phenomenological models, empirical constants arise, which have been adjusted by comparison to computational data. The disagreement between the present value of C_{ε_1} and that used in the standard (quasi-homogeneous) $k-\varepsilon$ model suggests that an element may be missing from the ε equation. That element would effectively cause a transition of C_{ε_1} from its near-wall value to its quasi-homogeneous value. It is quite likely that improvements to this and to other aspects of the model will be found.

Given the proliferation of eddy viscoscity damping functions (f_μ in Patel *et al.* (1985)) the present attempt at a more fundamental approach to the near-wall modeling problem would seem warranted. It is hoped that the present results indicate a possibility of its success.

Acknowledgment

I am grateful to Drs J. Kim and N. Mansour for discussing this work with me.

Appendix A. Possible Justification for the $\wp_{ij}$ Model

In the text the elliptic relaxation model was justified by the notion that some of the physical effects which are important in strongly inhomogeneous turbulent flows are governed by elliptic equations. Effects such as wall blocking or irrotational flow induced outside vortical regions (Gartshore *et al.*, 1983) are due to elliptic action at a distance.

In quasi-homogeneous models different regions of a turbulent flow are only allowed to communicate through parabolic diffusion across their boundaries. Just as these parabolic models are based on somewhat nebulous, intuitive grounds, so is the present model based largely on the suggestive reasoning given above and in the introduction.

This appendix describes some formal manipulations which might justify the type of model described by (13) and (B.7). For simplicity we work with the familiar "fast" pressure-strain tensor rather than with the function $\wp_{ij}$ defined below (B.1). These manipulations are only meant to be suggestive: the proper interpretation of $\wp_{ij}$ is somewhat vague, although its function in our model is not; as was explained in the text, the $\wp_{22}$ equation allows the kinematic wall blocking condition to be satisfied, even though blocking is not caused by pressure-strain correlations. The wall also has a direct influence on the pressure-strain term (Gibson and Launder, 1978); so, in addition to representing indirectly the suppression of the normal velocity component, the elliptic model also represents this direct effect.

In incompressible turbulence the fast pressure satisfies (in units such tht $\rho = 1$)

$$\nabla^2 p = -2\partial_k \bar{U}_l \partial_l u_k. \tag{A.1}$$

An equation for the fast pressure-strain correlation is obtained by multiplying (A.1) by the rate of strain $s_{ij} \equiv \frac{1}{2}(\partial_i u_j + \partial_j u_i)$ and averaging

$$\nabla^2 \overline{ps_{ij}} - \partial_k(\overline{p\partial_k s_{ij}}) - \overline{\partial_k p \partial_k s_{ij}} = -2\partial_k \bar{U}_l \overline{\partial_l u_k s_{ij}}. \tag{A.2}$$

It might be argued that $\overline{p\partial_k s_{ij}}$ can be neglected on the left-hand side of (A.2) because p is associated with large scales of turbulence while $\partial_k s_{ij}$ is associated with small scales: the reasoning is that disparate scales are uncorrelated. Unfortunately that reasoning can be misleading: the same line of thought would imply that $\overline{ps_{ij}}$ could be neglected in the Reynolds stress equations. The argument of scale separation is correct if applied to the *correlation coefficient*: $(\overline{ps_{ij}}^2/\overline{p^2}\,\overline{s_{ij}^2})^{1/2}$ does become negligible at high Reynolds number; but this reasoning does not justify dropping pressure-strain terms.

However, it seems likely that in strongly inhomogeneous regions the second term on the left-hand side of (A.2) will be small compared with the first. If that term is dropped, and if it is assumed that a scalar length can be defined such that

$$\overline{\partial_k p \partial_k s_{ij}} = \frac{\overline{ps_{ij}}}{L^2}, \tag{A.3}$$

then (A.2) takes an elliptic relaxation form

$$\nabla^2 \overline{ps_{ij}} - \frac{\overline{ps_{ij}}}{L^2} = -2\partial_k \bar{U}_l \overline{\partial_l u_k s_{ij}}. \tag{A.4}$$

The fact that we worked only with the fast pressure-strain is irrelevant to this justification of elliptic relaxation. Also s_{ij} could just as well have been defined as rate of strain divided by k, so that the pressure-strain would be normalized as in (13) and (B.3).

Another way of arriving at a relaxation model is to begin by inverting the Laplacian in (A.1) using the free-space Green's function:

$$p(\mathbf{x}) = \frac{1}{2\pi} \int \frac{\partial_k \bar{U}_l(\mathbf{x}') \partial_l u_k(\mathbf{x}')}{|\mathbf{x} - \mathbf{x}'|} d\mathbf{x}', \tag{A.5}$$

where the integral is over the flow and boundary contributions have been ignored. Multiplying by s_{ij} and averaging gives

$$\overline{ps_{ij}}(\mathbf{x}) = \frac{1}{2\pi} \int \frac{\partial_k \bar{U}_l(\mathbf{x}') \overline{\partial_l u_k(\mathbf{x}') s_{ij}(\mathbf{x})}}{|\mathbf{x} - \mathbf{x}'|} d\mathbf{x}'. \tag{A.6}$$

At this point the quasi-homogeneous approximation is usually made: the mean velocity derivative is taken outside the integral and the turbulence correlation is assumed to depend only on $|\mathbf{x} - \mathbf{x}'|$. With those simplifications (A.6) becomes $\overline{ps_{ij}} = A_{ijkl} \partial_k \bar{U}_l$ (Lumley, 1978) where $\mathbf{A}$ is a constant tensor. Suppose instead that we assume the turbulence correlation function is exponential, so that (A.6) becomes

$$\overline{ps_{ij}}(\mathbf{x}) = \frac{1}{2\pi} \int \partial_k \bar{U}_l(\mathbf{x}') \overline{\partial_l u_k s_{ij}}(\mathbf{x}') \frac{e^{-|\mathbf{x}-\mathbf{x}'|/L}}{|\mathbf{x} - \mathbf{x}'|} d\mathbf{x}'. \tag{A.7}$$

The operator

$$\int \frac{e^{-|\mathbf{x}-\mathbf{x}'|/L}}{4\pi |\mathbf{x} - \mathbf{x}'|} (\cdot)\, d\mathbf{x}', \tag{A.8}$$

where $(\cdot)$ represents a function of $\mathbf{x}'$, has inverse $\nabla^2 - L^{-2}$, i.e.,

$$\left(\frac{1}{r^2} d_r r^2 d_r - \frac{1}{L^2}\right)\left(\frac{e^{-r/L}}{4\pi r}\right) = -\delta(r).$$

Applying this inversion to (A.7) gives

$$\nabla^2 \overline{ps_{ij}} - \frac{\overline{ps_{ij}}}{L^2} = -2\partial_k \bar{U}_l \overline{\partial_l u_k s_{ij}},$$

so this is another way of arriving at (A.4).

Appendix B. Tensor Form of the Model

A model of the LRR type (with an eddy viscoscity hypothesis) uncouples the k, ε, and $\overline{v^2}$ equations from the other components of the Reynolds stress tensor. In this appendix we explain how the present approach can be extended to these other components. This might help to clarify some aspects of the model; for instance it is shown how the Rotta anisotropic dissipation term enforces the viscous boundary condition (see (B.4) and (B.5)). This appendix might also give some idea of how the present considerations relate to other flows.

In channel flow the correlation tensor for the turbulent velocity satisfies

$$d_y\left(\nu + \frac{\nu_t}{\sigma_k}\right) d_y \overline{u_i u_j} - \overline{u_i u_j}\frac{\varepsilon}{k} = -\wp_{ij} + \overline{u_i v} d_y \bar{U}_j + \overline{u_j v} d_y \bar{U}_i, \tag{B.1}$$

where

$$\wp_{ij} = -\frac{\overline{u_i \partial_j p} + \overline{u_j \partial_i p}}{\rho} - \varepsilon_{ij} + \overline{u_i u_j}\frac{\varepsilon}{k}.$$

The dissipation term on the left-hand side of (B.1) is written in Rotta's anisotropic form (1). Note that the trace of $\wp_{ij}$ is (using the summation convention for repeated indices)

$$\wp_{ii} = -2\partial_i \overline{u_i p} \tag{B.2}$$

because $\varepsilon_{ii} = 2\varepsilon$ and $\partial_i u_i = 0$ if the turbulence is incompressible. The right-hand side of (B.2) is usually set to zero in models (the rationale sometimes given is that this term is lumped into "turbulent diffusion"). Mansour *et al.* (1988) found that in channel flow the right-hand side of (B.2) is indeed negligible.

In order for $\overline{v^2}$ to be $O(y^4)$ as $y \to 0$, we insisted in the text that $\wp_{22}$ have its correct behavior, $\wp_{22} \to O(y^2)$. The other diagonal velocity components are $O(y^2)$ as $y \to 0$. This behavior will be obtained correctly if the corresponding components of $\wp_{ij}$ are $o(1)$ as $y \to 0$; it is not otherwise necessary that these components of $\wp_{ij}$ be of correct order in y. (Our present approach does not correctly give $\overline{uv} \to O(y^3)$.) We therefore continue to write

$$\wp_{ij} = k f_{ij} \tag{B.3}$$

and need not worry that this makes all components of $\wp_{ij}$ be $O(y^2)$.

As $y \to 0$, (B.1) becomes (see (10))

$$d_y^2 \overline{u_i u_j} - 2\frac{\overline{u_i u_j}}{y^2} = o(1). \tag{B.4}$$

This has solution

$$\overline{u_i u_j} = A_{ij} y^2 + \frac{B_{ij}}{y} + o(y^2). \tag{B.5}$$

This viscous boundary condition is that $\overline{u_i u_j} \to y^2 \varepsilon_{ij}(0)/2\nu$ as $y \to 0$, so we see that $B_{ij} = 0$ and $A_{ij} = \varepsilon_{ij}(0)/2\nu$ where $\varepsilon_{ij}(0)$ is the dissipation tensor at the wall: $\varepsilon_{22}(0) = 0$ was used implicitly in the text.

This wall boundary condition to (B.1) requires that $\varepsilon_{ij}(0)$ be modeled. We can use the standard

tensor invariance approach (Lumley, 1978), but the velocity anisotropy cannot enter the model: in fact A_{ij} determines this anisotropy, and A_{ij} is what is being modeled. It makes sense to assume that $\varepsilon_{ij}(0)$ is a function of the wall shear, since the time-scale of the mean shear is shorter than the eddy time-scales near the wall. Thus, we propose the form

$$\varepsilon_{ij}(0) = \varepsilon \Phi_{ij}(\partial_k \bar{U}_l(0), \delta_{kl}).$$

The simplest form for the tensor function Φ_{ij} that has the correct behavior is

$$\Phi_{ij} = \alpha \left[\frac{\partial_q \bar{U}_i \partial_q \bar{U}_j}{\partial_k \bar{U}_l \partial_k \bar{U}_l} \right] + \left(1 - \frac{\alpha}{2}\right) \left[\delta_{ij} - \frac{\partial_i \bar{U}_q \partial_j \bar{U}_q}{\partial_k \bar{U}_l \partial_k \bar{U}_l} \right] \tag{B.6}$$

(with summation over repeated indices). This satisfies $\varepsilon_{ii} = 2\varepsilon$ and in a channel $\varepsilon_{2j} = 0$ at the walls. The computations of Mansour *et al.* (1988) suggest $\alpha \approx 1$. This gives $\varepsilon_{11}(0)/\varepsilon_{33}(0) = 3$, which is about the value found in the numerical simulations.

In analogy to (13) of the text, f_{ij} satisfies an elliptic relaxation model

$$L^2 d_y^2 f_{ij} - f_{ij} = -\frac{\Pi_{ij}}{k} - \frac{[\overline{u_i u_j}/k - 2/3\delta_{ij}]}{T}, \tag{B.7}$$

where Π_{ij} is a model, such as the LRR pressure-strain model, to which $\wp_{ij}$ relaxes in the homogeneous limit. Equation (B.1) in combination with (B.7) provides a fourth-order ordinary differential equation for $\overline{u_i u_j}$ to which suitable boundary conditions can be applied.

References

Gartshore, I.S., Durbin, P.A., and Hunt, J.C.R. (1983) The production of turbulent stress in a shear flow by irrotational fluctuations. *J. Fluid Mech.* **193**, 475–497.

Gibson M.M., and Launder, B.E. (1978) Ground effects on pressure fluctuations in the atmospheric boundary layer. *J. Fluid Mech.* **86**, 491–511.

Hanjalic, K., and Launder, B.E. (1976) Contribution towards a Reynolds-stress closure for low-Reynolds-number turbulence. *J. Fluid Mech.* **74**, 593–610.

Hunt, J.C.R., and Graham, J.M.R. (1978) Free-stream turbulence near plane boundaries. *J. Fluid Mech.* **84**, 209–235.

Kim, J., Moin, P., and Moser, R. (1978) Turbulence statistics in fully developed channel flow at low Reynolds number. *J. Fluid Mech.* **177**, 133–166.

Launder, B.E. (1986) Low Reynolds Number Turbulence Near Walls. Report TFD/86/4, Dept. of Mech. Eng., UMIST, Manchester.

Launder, B.E., Reece, G.J., and Rodi, W. (1975) Progress in the development of a Reynolds-stress turbulence closure. *J. Fluid Mech.* **68**, 537–566.

Lumley, J.L. (1978) Computational modelling of turbulent flows. *Adv. Appl. Mech.* **18**, 126–176.

Mansour, N.N., Kim, J., and Moin, P. (1988) Reynolds-stress and dissipation-rate bundgets in a turbulent channel flow. *J. Fluid Mech.* **194**, 15–44.

Mansour, N.N., Kim, J., and Moin, P. (1989) Near-wall $k - \varepsilon$ turbulence modeling. *AIAA J.* **27**, 1068–1073.

Patel, V.C., Rodi, W., and Scheurer, W. (1985) Turbulence models for near-wall and low Reynolds number flows: a review. *AIAA J.* **23**, 1308–1319.

Rodi, W. (1976) A new algebraic relation for calculating the Reynolds stresses. *Z. Argew. Math. Mech.* **56**, T219–221.

Rotta, J.C. (1951) Statistische theorie nichthomogener turbulenz. *Z. Phys.* **129**, 547–572.

Shih, T.H. (1990) An improved $k - \varepsilon$ model for near wall turbulence and comparison with direct numerical simulations. In preparation

Thomas, N.H., and Hancock, P.E. (1977) Grid turbulence near a moving wall. *J. Fluid Mech.* **82**, 481–496.

Townsend, A.A. (1976) *The Structure of Turbulent Shear Flow*, Cambridge University Press, Cambridge.

van Driest, E.R. (1956) On turbulent flow near a wall. *J. Aero. Sci.* **23**, 1007–1011.